(2E)-1-(5-chlorothiophen-2-yl)-3-{4-[(E)-2-phenylethenyl] phenyl}prop-2-en-1-one : Synthesis, XRD, FT-IR, Raman and DFT studies

ARTICLE *in* SPECTROCHIMICA ACTA PART A MOLECULAR AND BIOMOLECULAR SPECTROSCOPY · OCTOBER 2015

Impact Factor: 2.35 · DOI: 10.1016/j.saa.2015.04.022

Spectrochimica Acta Part A: Molecular and Biomolecular Spectroscopy 149 (2015) 385–395

Contents lists available at ScienceDirect

Spectrochimica Acta Part A: Molecular and Biomolecular Spectroscopy

journal homepage: www.elsevier.com/locate/saa

(2*E*)-1-(5-Chlorothiophen-2-yl)-3-{4-[(*E*)-2-phenylethenyl]phenyl} prop-2-en-1-one: Synthesis, XRD, FT-IR, Raman and DFT studies

Cemal Parlak [a], Ponnadurai Ramasami [b], Chandraju Sadolalu Chidan Kumar [c,d,*], Mahir Tursun [a], Ching Kheng Quah [c], Lydia Rhyman [b], Metin Bilge [f], Hoong-Kun Fun [c,e], Siddegowda Chandraju [g]

[a] Department of Physics, Dumlupinar University, Kütahya 43100, Turkey
[b] Computational Chemistry Group, Department of Chemistry, Faculty of Science, University of Mauritius, Réduit 80837, Mauritius
[c] X-ray Crystallography Unit, School of Physics, Universiti Sains Malaysia, 11800 USM Penang, Malaysia
[d] Department of Engineering Chemistry, Alva's Institute of Engineering & Technology, Visvesvaraya Technological University, Moodbidri 574225, Karnataka, India
[e] Department of Pharmaceutical Chemistry, College of Pharmacy, King Saud University, Riyadh 11451, Saudi Arabia
[f] Department of Physics, Science Faculty, Ege University, İzmir 35100, Turkey
[g] Department of Sugar Technology and Chemistry, Sir M. Visvesvaraya PG Center, University of Mysore, Tubinakere, Mandya 571402, India

HIGHLIGHTS

- The conformation of the title compound was investigated by experimental and theoretical methods.
- 3D structure was confirmed by single crystal XRD data.
- The experimental results were supported by computational studies using DFT.
- Theoretical calculations are in good agreement with the experimental results.

GRAPHICAL ABSTRACT

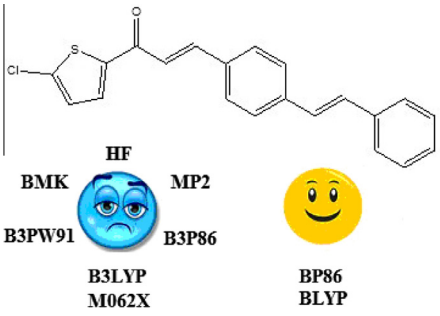

ARTICLE INFO

Article history:
Received 5 November 2014
Received in revised form 18 December 2014
Accepted 14 April 2015
Available online 28 April 2015

Keywords:
5-Chlorothiophene chalcone analogues
Crystal structures
Vibrational spectra
XRD
DFT

ABSTRACT

A novel (2*E*)-1-(5-chlorothiophen-2-yl)-3-{4-[(*E*)-2-phenylethenyl]phenyl}prop-2-en-1-one [$C_{21}H_{15}ClOS$] compound has been synthesized and its structure has been characterized by FT-IR, Raman and single-crystal X-ray diffraction techniques. The conformational isomers, optimized geometric parameters, normal mode frequencies and corresponding vibrational assignments of the compound have been examined by means of HF, MP2, BP86, BLYP, BMK, B3LYP, B3PW91, B3P86 and M06-2X functionals. Reliable vibrational assignments and molecular orbitals have been investigated by the potential energy distribution and natural bonding orbital analyses, respectively. The compound crystallizes in the triclinic space group *P*-1 with the *cis–trans–trans* form. There is a good agreement between the experimentally determined structural parameters and vibrational frequencies of the compound and those predicted theoretically using the density functional theory with the BLYP and BP86 functionals.

Introduction

Scientific studies of chalcones have attracted researchers. Chalcones represent an essential group of natural as well as synthetic products. Chalcone forms an important group of natural compounds with the ease to synthesize. They are known to be important

* Corresponding author at: Department of Engineering Chemistry, Alva's Institute of Engineering & Technology, Visvesvaraya Technological University, Moodbidri 574225, Karnataka, India. Tel.: +60 164930640.
E-mail address: chidankumar@gmail.com (C.S.C. Kumar).

http://dx.doi.org/10.1016/j.saa.2015.04.022
1386-1425/

precursors and valuable intermediates in the synthesis of active pharmaceutical drugs and biosynthesis of flavonoids. Researchers reported several methods for the synthesis of chalcones. Among them, aldol condensation and Claisen–Schmidt condensation between aryl ketones and aromatic aldehydes in acidic or basic media still occupy prominent positions. Chalcones are characterized by possessing two aryl rings that are linked *via* aliphatic three carbon chain. Introduction of various substituents into the two aryl rings is also a subject of interest because it leads to useful structure–activity relationship (SAR). Chalcones and their derivatives are proven to exhibit pharmacological activities such as antibacterial [1], antitumour [2], anticancer [3], antitubercular [4], anti-inflammatory [5], antioxidant [6] and antimalarial [7]. The synthesis and spectroscopic characterization of novel thiophene chalcone analogs were reported by many research groups [8–11]. Some of us have earlier reported the X-ray crystal structures of few chalcone derivatives of 2,5-dichlorothiophene [12–14]. However, literature revealed that theoretical studies of chalcone compounds are limited, wherein, the first theoretical study on the structural and spectral aspects of 4-bromo-1-naphthyl chalcone was reported by Nithya and coworkers [15] in 2011.

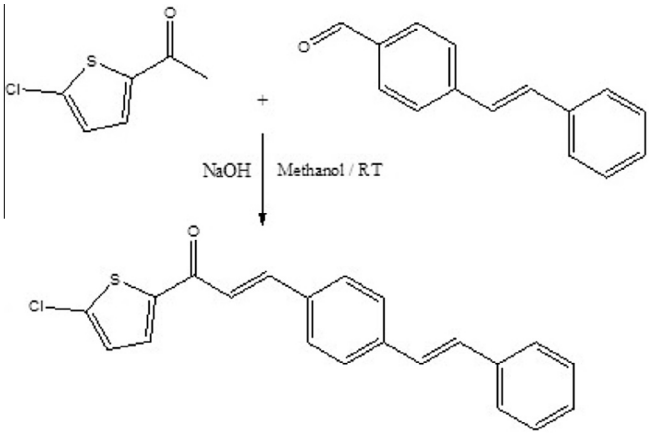

Fig. 1. Synthesis of (2*E*)-1-(5-chlorothiophen-2-yl)-3-{4-[(*E*)-2-phenylethenyl]phenyl}prop-2-en-1-one.

Continuing with our interest in the synthesis of 5-chlorothiophene chalcone compounds [16–18], in the present study, (2*E*)-1-(5-chlorothiophen-2-yl)-3-{4-[(*E*)-2-phenylethenyl] phenyl}prop-2-en-1-one was synthesized by reacting 2-acetly-5-chlorothiophene with 4-styryl-benzaldehyde (Fig. 1) in basic medium. The structure of the compound was characterized by FT-IR, Raman and confirmed by single crystal X-ray diffraction (XRD) studies. In addition, DFT method in conjunction with the BP86 and BLYP functionals using 6-31G(d) basis set was employed to predict the structural and spectroscopic parameters of the compound in the gas phase. The findings of these spectroscopic and theoretical studies are herein reported.

Experimental

Instrumentation

FT-MIR and FT-FIR spectra of the title compound were recorded by KBr pellet technique in the region of 4000–400 cm^{-1} and 400–40 cm^{-1} with Bruker Optics IFS66v/s FT-IR spectrometer at a resolution of 2 cm^{-1}, respectively. Raman spectrum was obtained using a Bruker Senterra Dispersive Raman microscope spectrometer with 532 nm excitation from a 3B diode laser having 2 cm^{-1} resolution in the spectral region of 4000–40 cm^{-1}.

A yellow, block-shaped single crystal of the title compound, with dimensions of 0.629 × 0.259 × 0.099 mm was selected and mounted on a Bruker APEX II DUO CCD diffractometer with a fine-focus sealed tube graphite-monochromated Mo Kα radiation (λ = 0.71073 Å) at 296 K in the range of $2.35° \leqslant \theta \leqslant 29.95°$. The data was processed with SAINT and corrected for absorption using SADABS. A total of 36201 reflections were collected, of which 10028 reflections were independent and 6202 reflections with $I > 2\sigma(I)$. The structure was solved by direct method using the program SHELXTL and was refined by full-matrix least squares technique on F^2 using anisotropic displacement parameters for all non-hydrogen atoms. All the hydrogen atoms were located from the difference Fourier map and refined freely with fixed isotropic displacement parameters. 4-Styryl benzene moiety of one of the molecules is disordered over two sites with refined site occupancies ratio 0.558(8):0.442(8). The final full-matrix least squares

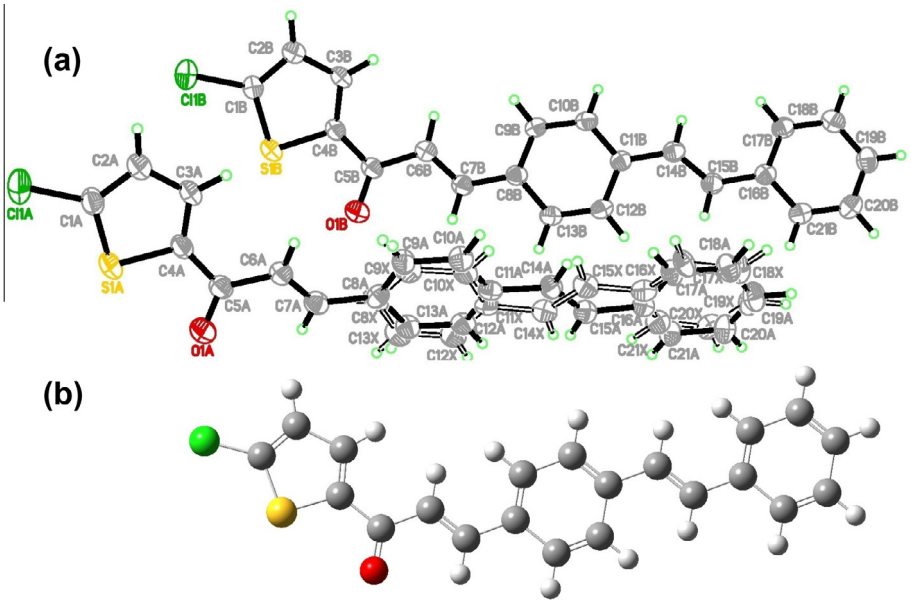

Fig. 2. (a) The molecular structure of compound showing 30% probability displacement ellipsoids and the atom numbering scheme. The minor disorder component is indicated with open bonds. (b) Optimized structure of *cis–trans–trans* isomer.

Table 1
Some features in various methods for the *cis–trans–trans* conformer of the compound.

Method	Symmetry	ΔG (Hartree)	Imaginary frequency	Dipole moment	Relative stability (kcal/mol)	Mole fractions (%)
HF/6-31G(d)	C_1	−1735.527631	2	5.6606	0.00	50.2
	C_s	−1735.527622	2	5.6605	0.01	49.8
MP2/6-31G(d)	C_1	−1738.636965	3	4.6166	0.00	50
	C_s	−1738.636965	3	4.6167	0.00	50
BP86/6-31G(d)	C_1	−1742.663046	0	5.5801	1.44	8
	C_s	−1742.665347	0	5.5787	0.00	92
BP86/6-311+G(3df,p)	C_1	−1743.009688	0	5.2959	0.00	65.2
	C_s	−1743.009095	1	5.2949	0.37	34.8
BLYP/6-31G(d)	C_1	−1742.215487	0	5.6277	1.07	14.1
	C_s	−1742.217195	0	5.6265	0.00	85.9
BMK/6-31G(d)	C_1	−1741.743351	0	5.5114	0.00	99
	C_s	−1741.739124	1	5.5077	2.65	1
B3LYP/6-31G(d)	C_1	−1742.607044	0	5.4646	0.00	85.7
	C_s	−1742.605356	1	5.4639	1.06	14.3
B3LYP/6-311+G(3df,p)	C_1	−1742.958875	0	5.1955	0.00	100
	C_s	−1742.946970	1	5.1951	7.47	0
B3P86/6-31G(d)	C_1	−1745.914187	0	5.4322	0.00	81.7
	C_s	−1745.912776	1	5.4313	0.89	18.3
B3PW91/6-31G(d)	C_1	−1742.164468	0	5.4174	0.00	85.5
	C_s	−1742.162798	1	5.4161	1.05	14.5
M06-2X/6-31G(d)	C_1	−1742.155165	2	4.9835	0.00	65.9
	C_s	−1742.154544	3	4.9878	0.39	34.1

refinement gave $R = 0.051$ and $wR = 0.168$, $S = 1.017$, $\Delta\rho_{max} = 0.23$ e Å^{-3} and $\Delta\rho_{min} = -0.23$ e Å^{-3}.

Synthesis

2-Acetly-5-chlorothiophene (0.01 mol) and 4-styryl-benzaldehyde (0.01 mol) were dissolved in 20 ml methanol (Fig. 1). A catalytic amount of NaOH was added to the solution dropwise with vigorous stirring. The reaction mixture was stirred for about 5–6 h at room temperature. The resulting crude products were filtered, washed successively with distilled water and recrystallized from ethanol to get the title chalcone. Crystals suitable for X-ray diffraction studies were obtained from acetone/ethanol (1:1 v/v) mixture by slow evaporation technique at room temperature.

Computational details

All the computations were performed using Gaussian 09 program package [19] and GaussView [20] was used for visualization of the structure and simulation of the vibrational spectra. Starting geometry of the compound (*cis–trans–trans*) for the computations was taken from X-ray refinement data (Fig. 2). Conformational isomers were identified as *cis* and *trans* with respect to the O/S atoms, C6═C7 and C14═C15 bonds of the compound [16–18,21–23].

For all computations, the *cis–trans–trans* isomer without symmetry and C_s symmetry were optimized using HF and MP2 methods and the BP86, BLYP, BMK, B3LYP, B3PW91, B3P86 and M06-2X functionals in conjunction with the 6-31G(d) basis set in the gas phase. The optimizations were also conducted using the 6-311+G(3df,p) basis set for B3LYP and BP86 functionals. The eight conformers in C_s symmetry were optimized using BP86/6-31G(d) and BLYP/6-31G(d) methods in the gas phase.

Harmonic vibrational frequencies and their corresponding vibrational intensities, scaled by 0.9914 and 0.9940 [24], were also computed by the BP86 and BLYP functionals with 6-31G(d) basis set. The fundamental normal modes were assigned. Potential energy distribution (PED) calculations were carried out by the

Table 2
Energetic of the eight conformers of the compound.

Conformational isomer (C_s)	ΔG (Hartree)	Imaginary frequency	Relative stability (kcal/mol)	Mole fraction (%)
BP86/6-31G(d)				
Cis–Cis–Cis	−1742.634644	1	19.27	0
Cis–Cis–Trans	−1742.656774	0	5.38	0
Cis–Trans–Cis	−1742.641803	2	14.77	0
Cis–Trans–Trans	−1742.665347	0	0.00	87.3
Trans–Trans–Cis	−1742.633882	2	19.74	0
Trans–Cis–Trans	−1742.653164	1	7.64	0
Trans–Trans–Cis	−1742.640736	2	15.44	0
Trans–Trans–Trans	−1742.663530	0	1.14	12.7
BLYP/6-31G(d)				
Cis–Cis–Cis	−1742.186983	2	18.96	0
Cis–Cis–Trans	−1742.209294	0	4.96	0
Cis–Trans–Cis	−1742.194158	2	14.46	0
Cis–Trans–Trans	−1742.217195	0	0.00	91.4
Trans–Trans–Cis	−1742.186064	2	19.53	0
Trans–Cis–Trans	−1742.208748	0	5.30	0
Trans–Trans–Cis	−1742.192942	2	15.22	0
Trans–Trans–Trans	−1742.214968	0	1.40	8.6

Table 3
Crystal data and parameters for structure refinement of the compound.

Features	Compound
CCDC	948857
Molecular formula	$C_{21}H_{15}ClOS$
Molecular weight	350.84
Crystal system	Triclinic
Space group	*P*-1
T, *K*	296
Z	4
a (Å)	5.9977(5)
b (Å)	8.4299(7)
c (Å)	34.761(3)
α (°)	91.509(2)
β (°)	94.169(2)
γ (°)	100.444(2)
V (Å^3)	1722.4(3)
D_{calc} (g cm^{-3})	1.353
μ (mm^{-1})	0.347
Reflections measured	10028
Ranges/indices (*h*, *k*, *l*)	−8, 8; −11, 11; −48, 48
θ limit (°)	1.76–30.11
Completeness, %	98.7
Observed reflections ($I > 2\sigma(I)$)	6202
T_{min}, T_{max}	0.8114, 0.9665
Goodness of fit on F^2	1.017
R_{int}, R_1, wR_2	0.031, 0.051, 0.168

VEDA 4 (Vibrational Energy Distribution Analysis) as described earlier [25]. Calculated Raman activities were converted to relative Raman intensities using the relationship derived from the intensity theory of Raman scattering [23,26,27]. The highest occupied and lowest unoccupied molecular orbitals (HOMO and LUMO) of the compound were analyzed. Natural bond orbital (NBO) analysis was also used to have more insights in the nature of bonding [28,29].

Results and discussion

The results of the electronic computations on the isomers and geometrical parameters of the synthesized compound are reported and discussed with respect to the X-ray data. This is followed by discussion of the experimental and theoretical vibrational frequencies and their intensities. The molecular orbitals are also explored.

Geometrical structures

The energetic, imaginary frequency and dipole moment of the *cis–trans–trans* isomer are listed in Table 1. For both symmetries, the vibrational analysis shows imaginary frequency except with the BP86 and BLYP functionals and the 6-31G(d) basis set. It is surprising that larger basis sets do not perform well. We considered only those structures not giving imaginary frequency. The *cis–trans–trans* isomer in C_s symmetry is more stable than C_1 by 1.44 and 1.07 kcal/mol for the BP86/6-31G(d) and BLYP/6-31G(d) methods, respectively. The *cis–trans–trans* conformer in the gas phase prefers C_s and C_1 symmetries with the approximate percentage of 92 and 8 with BP86 and 86 and 14 with BLYP functionals, respectively [23,26,27,30].

The optimized energies for eight conformers of the compound in C_s symmetry using BP86/6-31G(d) and BLYP/6-31G(d) are listed in Table 2. Regarding the calculated free energies, all forms except *trans–trans–trans* relative to the most stable form could be neglected for the calculation of equilibrium constant since their energy differences are larger than 2 kcal/mol [22,30]. The *cis–trans–trans* isomer is more stable than the *trans–trans–trans* isomer by a free energy difference of 1.14 and 1.40 kcal/mol, respectively. The compound in the gas phase prefers the *cis–trans–trans* and the conformers with the approximate preference of 87% and 12% for BP86 and 91% and 9% for BLYP functionals, respectively [23,26,27,30]. It is found that the molecule under investigation is most stable in *cis–trans–trans* form as reported in XRD results.

A summary of the crystal data and parameters of the compound for structure refinement details are given in Table 3. All other refinement details are available in the CIF (CCDC: 948857). The molecular structure of the compound showing 30% probability displacement ellipsoids and atom labelling scheme is depicted in Fig. 2. The asymmetric unit of the compound, contains two crystallographically

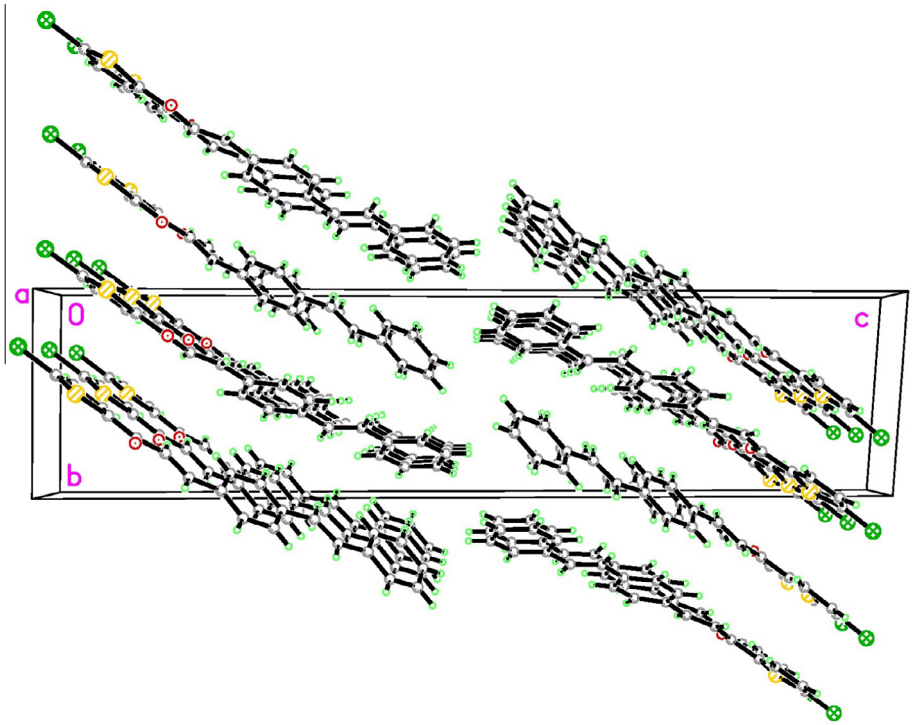

Fig. 3. Crystal packing of the compound, showing molecules stacked along *a*-axis.

Table 4
Experimental and theoretical geometrical parameters of the compound.

Bond lengths (Å)	Exp.	BLYP	BP86	Bond angles (°)	Exp.	BLYP	BP86	Bond angles (°)	Exp.	BLYP	BP86
C5B-C6B	1.478	1.485	1.480	C8B-C7B-H7BA	116.3	116.1	116.4	C19B-C20B-C21B	120.3	120.1	120.0
C5B-O1B	1.231	1.250	1.248	C7B-C8B-C13B	119.0	118.9	118.9	C19B-C20B-H20B	119.8	120.2	120.2
C5B-C4B	1.462	1.482	1.477	C7B-C8B-C9B	123.7	123.9	123.8	C21B-C20B-H20B	119.8	119.7	119.8
C6B-C7B	1.322	1.364	1.363	C13B-C8B-C9B	117.4	117.2	117.3	C16B-C21B-C20B	121.5	121.4	121.3
C6B-H6BA	0.930	1.093	1.096	C8B-C13B-C12B	122.0	121.8	121.7	C16B-C21B-H21B	119.2	118.9	118.9
C7B-C8B	1.463	1.460	1.456	C8B-C13B-H13B	119.0	118.7	118.7	C20B-C21B-H21B	119.2	119.7	119.8
C7B-H7BA	0.930	1.097	1.100	C12B-C13B-H13B	119.0	119.5	119.6	Torsion angles (°)	Exp.	BLYP	BP86
C8B-C13B	1.397	1.423	1.421	C13B-C12B-C11B	120.8	121.1	121	O1B-C5B-C6B-C7B	−16.0	0.0	0.0
C8B-C9B	1.397	1.422	1.419	C13B-C12B-H12B	119.6	119.0	119	C4B-C5B-C6B-C7B	163.8	180.0	180.0
C13B-C12B	1.374	1.395	1.393	C11B-C12B-H12B	119.6	120.0	120	C6B-C5B-C4B-C3B	5.0	0.0	0.0
C13B-H13B	0.930	1.095	1.097	C12B-C11B-C10B	117.3	117.1	117.2	C6B-C5B-C4B-S1B	−177.3	−180.0	−180.0
C12B-C11B	1.401	1.422	1.420	C12B-C11B-C14B	123.2	124.1	124	O1B-C5B-C4B-C3B	−175.2	−180.0	−180.0
C12B-H12B	0.930	1.093	1.095	C10B-C11B-C14B	119.5	118.8	118.8	O1B-C5B-C4B-S1B	2.5	0.0	0.0
C11B-C10B	1.396	1.424	1.422	C11B-C10B-C9B	121.8	121.8	121.8	C5B-C6B-C7B-C8B	−177.8	−180.0	−180.0
C11B-C14B	1.464	1.465	1.460	C11B-C10B-H10B	119.1	118.8	118.7	C6B-C7B-C8B-C13B	165.7	180.0	180.0
C10B-C9B	1.381	1.394	1.392	C9B-C10B-H10B	119.1	119.4	119.5	C6B-C7B-C8B-C9B	−14.7	0.0	0.0
C10B-H10B	0.930	1.095	1.097	C8B-C9B-C10B	120.7	121.0	120.9	C7B-C8B-C13B-C12B	−178.1	−180.0	−180.0
C9B-H9BA	0.930	1.093	1.095	C8B-C9B-H9BA	119.6	119.9	119.9	C9B-C8B-C13B-C12B	2.2	0.0	0.0
C4B-C3B	1.371	1.392	1.392	C10B-C9B-H9BA	119.6	119.1	119.2	C7B-C8B-C9B-C10B	179.9	180.0	180.0
C4B-S1B	1.720	1.774	1.759	C5B-C4B-C3B	131.2	132.6	132.6	C13B-C8B-C9B-C10B	−0.4	0.0	0.0
C3B-C2B	1.400	1.426	1.422	C5B-C4B-S1B	117.7	116.3	116.1	C8B-C13B-C12B-C11B	−1.8	0.0	0.0
C3B-H3BA	0.930	1.091	1.093	C3B-C4B-S1B	111.0	111.1	111.3	C13B-C12B-C11B-C10B	−0.4	0.0	0.0
C2B-C1B	1.350	1.385	1.385	C4B-C3B-C2B	113.3	113.9	113.7	C13B-C12B-C11B-C14B	−179.7	−180.0	−180.0
C2B-H2BA	0.930	1.091	1.092	C4B-C3B-H3BA	123.4	123.4	123.4	C12B-C11B-C10B-C9B	2.2	0.0	0.0
C1B-S1B	1.705	1.756	1.745	C2B-C3B-H3BA	123.4	122.7	122.9	C14B-C11B-C10B-C9B	−178.5	−180.0	−180.0
C1B-Cl1B	1.712	1.748	1.733	C3B-C2B-C1B	111.5	111.5	111.3	C12B-C11B-C14B-C15B	−10.2	0.0	0.0
C14B-C15B	1.326	1.365	1.364	C3B-C2B-H2BA	124.2	124.8	125.1	C10B-C11B-C14B-C15B	170.6	180.0	180.0
C14B-H14B	0.930	1.096	1.099	C1B-C2B-H2BA	124.2	123.6	123.5	C11B-C10B-C9B-C8B	−1.8	0.0	0.0
C15B-C16B	1.467	1.468	1.464	C2B-C1B-S1B	113.4	113.3	113.4	C5B-C4B-C3B-C2B	177.3	180.0	180.0
C15B-H15B	0.930	1.097	1.099	C2B-C1B-Cl1B	127.4	126.0	126	S1B-C4B-C3B-C2B	−0.5	0.0	0.0
C16B-C17B	1.397	1.421	1.419	S1B-C1B-Cl1B	119.2	120.7	120.6	C5B-C4B-S1B-C1B	−177.5	−180.0	−180.0
C16B-C21B	1.395	1.420	1.418	C4B-S1B-C1B	90.7	90.1	90.3	C3B-C4B-S1B-C1B	0.7	0.0	0.0
C17B-C18B	1.384	1.400	1.398	C11B-C14B-C15B	126.5	127.1	126.9	C4B-C3B-C2B-C1B	0.0	0.0	0.0
C17B-H17B	0.930	1.093	1.095	C11B-C14B-H14B	116.8	114.3	114.4	C3B-C2B-C1B-S1B	0.6	0.0	0.0
C18B-C19B	1.380	1.409	1.407	C15B-C14B-H14B	116.8	118.6	118.7	C3B-C2B-C1B-Cl1B	−179.9	−180.0	−180.0
C18B-H18B	0.930	1.094	1.096	C14B-C15B-C16B	127.2	127.4	127.2	C2B-C1B-S1B-C4B	−0.8	0.0	0.0
C19B-C20B	1.380	1.406	1.404	C14B-C15B-H15B	116.4	118.5	118.5	Cl1B-C1B-S1B-C4B	179.7	180.0	180.0
C19B-H19B	0.930	1.094	1.096	C16B-C15B-H15B	116.4	114.1	114.3	C11B-C14B-C15B-C16B	−178.2	−180.0	−180.0
C20B-C21B	1.373	1.402	1.400	C15B-C16B-C17B	123.3	123.7	123.6	C14B-C15B-C16B-C17B	3.9	0.0	0.0
C20B-H20B	0.930	1.094	1.096	C15B-C16B-C21B	119.3	118.6	118.6	C14B-C15B-C16B-C21B	−176.8	−180.0	−180.0
C21B-H21B	0.930	1.095	1.097	C17B-C16B-C21B	117.4	117.7	117.7	C15B-C16B-C17B-C18B	178.6	180.0	180.0
Bond angles (°)	Exp.	BLYP	BP86	C16B-C17B-C18B	120.9	120.9	120.9	C21B-C16B-C17B-C18B	−0.7	0.0	0.0
C6B-C5B-O1B	122.5	122.7	122.8	C16B-C17B-H17B	119.5	119.9	119.9	C15B-C16B-C21B-C20B	−179.1	−180.0	−180.0
C6B-C5B-C4B	117.6	117.9	117.8	C18B-C17B-H17B	119.5	119.2	119.2	C17B-C16B-C21B-C20B	0.2	0.0	0.0
O1B-C5B-C4B	119.9	119.4	119.4	C17B-C18B-C19B	120.4	120.5	120.5	C16B-C17B-C18B-C19B	0.2	0.0	0.0
C5B-C6B-C7B	120.5	120.4	119.9	C17B-C18B-H18B	119.8	119.5	119.6	C17B-C18B-C19B-C20B	0.7	0.0	0.0
C5B-C6B-H6BA	119.7	118.3	118.5	C19B-C18B-H18B	119.8	120.0	120	C18B-C19B-C20B-C21B	−1.2	0.0	0.0
C7B-C6B-H6BA	119.7	121.4	121.6	C18B-C19B-C20B	119.4	119.5	119.5	C19B-C20B-C21B-C16B	0.8	0.0	0.0
C6B-C7B-C8B	127.5	128.3	128.2	C18B-C19B-H19B	120.3	120.2	120.2				
C6B-C7B-H7BA	116.3	115.6	115.4	C20B-C19B-H19B	120.3	120.3	120.3				

independent molecules with similar geometries (Fig. 2) both of which exist in *trans* conformations with respect to the C6═C7 and C14═C15 bonds [bond lengths ranging from 1.322 to 1.326 Å]. 4-Styryl benzene moiety of molecule *B* is modeled as disordered over two sites rotated by 180° from one another with refined site occupancies ratio 0.558:0.442. The thiophene ring (S1A/C1A-C4A) of molecule *A* forms dihedral angles of 26.8° and 28.1° with the two benzene rings (C8A-C13A and C16A-C21A). The corresponding dihedral angles for molecule *B* are 30.5° and 36.5° [33.4° and 36.6° for minor component]. The dihedral angle between the two benzene rings for molecules *A* and *B* is 1.8° and 6.3° [3.4° for minor component], respectively. There are no classical intermolecular hydrogen bonds observed in the crystal structure. In the crystal packing, molecules are stacked along *a*-axis (Fig. 3). Molecules are consolidated by weak intermolecular C—H…π (C12X-H12C: 0.930 Å, H12C…Cg1: 2.840 Å, C12X…Cg1: 3.499 Å, ∠C12XH12CCg1: 128.0° and C20X-H20C: 0.930 Å, H20C…Cg2: 2.850 Å, C20X…Cg2: 3.585 Å, ∠C20XH20CCg2: 137.0°) interactions with H…*Cg* distances of 2.840 and 2.850 Å, where *Cg* are the centroid of the two benzene rings of minor components of molecule *B* (C8X-C13X and C16X-C21X).

To clarify the vibrational frequencies, it is essential to examine the geometry of the compound. A very small change in the geometry can potentially cause substantial variations in their frequencies. Some of the experimental and theoretical geometrical parameters (bond lengths, bond and torsion angles) are listed in Table 4. In general, the computed parameters are in good agreement with the reported experimental data. Regarding the computations, the largest difference between the experimental and calculated bond lengths (angles/torsion) is 0.167 Å (2.5°/16.2°) for BLYP/6-31G(d) and 0.170 Å (2.4°/16.2°) for BP86/6-31G(d). The root mean square deviation (RMSD), the mean absolute deviation (MAD) and the correlation (R^2) values between the experimental and calculated bond lengths, angles and torsion angles are found to be 0.10 Å – 0.08 Å –

Table 5
Comparison of the experimental and computed vibrational frequencies (cm^{-1}) of the compound.

Mode	Assignment			BLYP/6-31G(d)			BP86/6-31G(d)		
	PED (⩾10%)[a]	IR	Raman	ν[b]	I_{IR}[c]	I_R[c]	ν[b]	I_{IR}[c]	I_R[c]
1(A′)	νCH (99)			3142	5.18	45.83	3138	3.99	46.72
2(A′)	νCH (99)			3124	10.96	11.02	3119	9.21	11.30
3(A′)	νCH (93)		3116	3108	56.97	68.44	3103	52.15	76.49
4(A′)	νCH (87)			3103	7.30	23.45	3095	6.59	24.33
5(A′)	νCH (88)	3096		3100	40.44	3.92	3093	48.40	30.80
6(A′)	νCH (91)		3095	3098	32.99	32.23	3092	17.67	5.57
7(A′)	νCH (94)			3090	12.08	45.21	3085	4.25	41.37
8(A′)	νCH (85)			3089	2.94	2.82	3080	5.24	2.89
9(A′)	νCH (84)			3082	4.60	10.53	3076	4.89	3.86
10(A′)	νCH (89)			3080	0.79	19.72	3075	1.10	20.87
11(A′)	νCH (88)	3076		3076	26.48	9.79	3070	21.63	8.52
12(A′)	νCH (90)			3073	11.89	14.64	3068	9.71	14.55
13(A′)	νCH (96)		3058	3065	0.93	6.56	3053	1.05	7.44
14(A′)	νCH (94)	3052	3038	3059	32.33	4.50	3050	36.75	5.08
15(A′)	νCH (96)	3025	3008	3049	1.47	12.19	3041	1.35	12.79
16(A′)	νCO (73) + νCC (18)	1643		1626	213.06	176.94	1636	191.81	64.49
17(A′)	νCC (81) + νCO (13)		1633	1622	9.56	2897.05	1627	10.99	2843.06
18(A′)	νCC (84)	1585		1591	31.74	530.91	1600	14.40	486.84
19(A′)	νCC (87)		1586	1577	9.44	9077.46	1587	31.70	5760.47
20(A′)	νCC (81)			1559	10.98	9.17	1566	107.35	2532.76
21(A′)	νCC (87)	1554	1557	1549	690.86	27808.95	1562	668.08	31169.98
22(A′)	νCC (80) + δCH (11)	1526	1526	1520	155.49	6322.89	1529	125.67	5378.60
23(A′)	νCC (82) + δCH (14)	1511		1510	43.77	67.36	1514	62.48	71.22
24(A′)	νCC (89)	1494		1501	21.99	0.41	1497	35.68	1.32
25(A′)	νCC (90)		1493	1487	1.04	710.73	1481	1.90	564.04
26(A′)	δCH (73) + νCC (19)	1449	1453	1444	18.16	716.83	1438	15.44	573.84
27(A′)	δCH (61) + νCC (29)			1418	42.29	63.88	1422	511.69	1541.11
28(A′)	νCC (89)	1420	1424	1410	477.38	1717.12	1418	12.29	18.28
29(A′)	δCH (89)			1352	56.84	9.16	1358	71.99	17.82
30(A′)	δCH (88)			1333	5.24	2995.12	1345	49.41	501.85
31(A′)	δCH (93)	1333	1327	1332	150.41	336.57	1321	82.20	781.10
32(A′)	δCH (94)			1329	57.27	1844.72	1319	189.80	1867.95
33(A′)	δCH (91)			1316	1.42	1363.45	1312	17.39	518.02
34(A′)	δCH (72) + νCC (23)	1294		1308	108.27	24.72	1308	5.92	1474.30
35(A′)	νCC (65) + δCH (29)			1304	3.57	15.42	1297	3.66	3.65
36(A′)	δCH (73) + νCC (15)	1269		1289	24.17	67.63	1284	15.23	16.38
37(A′)	νCC (88)		1269	1268	1.63	16.61	1274	2.09	52.24
38(A′)	δCH (71) + νCC (21)			1233	0.94	7.47	1227	6.65	33.41
39(A′)	δCH (90)		1228	1210	0.73	35.60	1206	211.05	265.30
40(A′)	δCH (83)	1224		1205	126.35	22.78	1199	41.33	25.44
41(A′)	δCH (82)			1189	27.71	158.57	1189	1.50	1793.34
42(A′)	δCH (84)	1176		1179	100.35	940.88	1178	74.94	314.07
43(A′)	δCH (85)			1179	18.59	56.03	1170	9.09	1252.56
44(A′)	νCC (87)	1157	1180	1168	204.14	12495.18	1165	88.20	8404.02
45(A′)	δCH (82)			1158	1.24	133.01	1150	0.14	22.93
46(A′)	δCH (76) + νCC (15)	1116		1110	7.20	11.34	1104	6.59	0.50
47(A′)	δCH (72)		1082	1076	3.75	20.07	1074	5.44	10.78
48(A′)	δCH (81) + νCC (11)	1074	1060	1068	70.29	10.17	1069	52.70	19.72
49(A′)	δCC (88)	1018	1028	1019	1.52	75.79	1020	2.00	105.21
50(A″)	γCH (86)	986		995	15.21	5.11	989	12.29	0.32
51(A′)	δCC (83)			993	0.93	8.55	985	18.92	5.19
52(A′)	δCC (79)		998	979	0.52	812.03	984	241.68	98.90
53(A′)	δCC (81)	967	967	972	270.23	236.80	974	2.02	688.54
54(A″)	γCH (91)			970	26.08	0.17	959	30.06	0.28
55(A″)	γCH (92)			946	2.22	5.29	949	28.72	740.63
56(A′)	δCC (88)		936	937	16.37	596.32	939	4.58	4.74
57(A″)	γCH (80)		919	924	0.28	8.98	915	0.55	8.85
58(A″)	γCH (86)			917	0.02	0.53	912	0.01	0.20
59(A″)	γCH (89)			912	0.10	0.21	907	0.10	0.26
60(A″)	γCH (78)	885	886	885	0.28	13.35	877	0.20	12.67
61(A′)	δCC (93)	864	861	867	9.73	257.29	868	7.75	214.78
62(A″)	γCH (73)			852	2.52	12.68	846	0.73	177.95
63(A′)	δCC (93)			848	1.11	207.61	844	2.59	13.30
64(A″)	γCH (87)			847	0.50	7.78	839	0.60	6.88
65(A″)	γCH (96)			836	1.54	29.03	829	2.09	28.92
66(A″)	γCH (91)	820		813	4.22	10.13	810	2.22	51.75
67(A′)	δCC (92)		818	809	1.76	38.53	806	5.28	10.08
68(A′)	δCC (94)			802	6.12	10.55	794	10.99	8.38
69(A″)	γCH (91)	798		800	32.39	3.91	792	33.35	5.88
70(A″)	γCH (88)	751		766	30.60	2.37	758	36.72	2.28
71(A″)	γCH (85)			744	5.38	3.42	738	4.44	3.14
72(A′)	δCO (64) + δCC (24)	729	745	735	64.78	50.45	735	71.11	23.58
73(A″)	γCH (89)			717	20.14	1.62	712	23.61	1.58

Table 5 (*continued*)

Mode	Assignment			BLYP/6-31G(d)			BP86/6-31G(d)		
	PED (⩾10%)[a]	IR	Raman	ν^{b}	I_{IR}^{c}	I_{R}^{c}	ν^{b}	I_{IR}^{c}	I_{R}^{c}
74(A′)	νCS (65) + δCC (23)	690	681	691	4.22	118.37	703	1.44	94.65
75(A″)	γCH (92)			678	5.67	8.31	673	6.70	8.25
76(A″)	γCH (87)			671	13.36	0.05	667	17.67	0.20
77(A′)	νCS (58) + δCO (28)	645	644	650	5.97	746.32	656	2.58	655.43
78(A′)	δCC (85)		622	634	1.35	55.37	629	2.36	79.44
79(A′)	δCC (81)	616		615	20.16	17.50	609	29.95	29.64
80(A′)	δCC (84)			612	24.36	97.44	606	11.99	83.32
81(A″)	γCC (68)			541	0.31	0.88	540	0.09	0.72
82(A′)	δCC (87)		547	533	1.70	60.31	529	3.41	73.82
83(A″)	γCH (85)	531		528	13.94	0.11	522	18.39	0.09
84(A′)	νCCl (69) + δCC (19)	513	506	499	19.45	78.05	501	22.08	64.16
85(A′)	δCC (87)	484	485	481	3.54	19.78	478	3.99	55.99
86(A″)	γCC (84)			477	0.23	0.73	471	0.62	0.90
87(A″)	γCC (68)	460	455	452	2.19	2.04	454	2.42	1.83
88(A′)	δCC (83)	436	433	450	16.37	55.50	447	15.14	64.49
89(A″)	γCC (48)	424		397	0.00	0.00	393	0.01	0.00
90(A′)	δCC (90)		407	395	0.03	0.10	390	0.04	0.10
91(A′)	δCS (70) + νCCl (22)	380	382	373	11.32	240.35	375	8.45	215.39
92(A″)	γCC (78)			366	0.31	6.00	364	0.36	5.92
93(A′)	δCC (64)	318	318	307	16.22	161.96	305	17.05	164.29
94(A′)	δCCl (68) + δCO (27)		260	274	4.45	197.15	273	4.62	217.57
95(A″)	τCCCCl (86)			258	0.31	8.49	258	0.44	16.79
96(A″)	τCCCC (74)			255	0.32	55.84	253	0.20	45.83
97(A′)	δCC (79)	228		231	4.27	13.98	230	3.17	3.79
98(A′)	δCC (68) + δCO (27)	190		216	2.86	4.39	214	4.09	11.71
99(A″)	τCCCC (66)	176	221	207	0.03	24.64	205	0.01	25.60
100(A″)	γCCl (68) + γCH (27)	138		139	0.02	55.90	138	0.03	57.49
101(A′)	δCC (69)	125		134	2.31	13.81	132	2.22	12.28
102(A′)	δCC (58)			120	1.58	101.15	119	1.93	90.50
103(A″)	τCCCO (71)	107		106	1.40	12.47	106	1.28	9.69
104(A″)	τCCCC (77)			95	0.07	32.42	93	0.01	33.03
105(A″)	τCCCC (74)			69	0.29	70.23	67	0.35	82.47
106(A′)	δCC (86)			62	0.06	168.47	62	0.06	169.27
107(A″)	τCCCC (82)			36	0.07	393.56	35	0.08	388.75
108(A″)	τHCCC (77)			28	0.62	294.47	27	0.72	287.03
109(A′)	δCC (89)			24	0.02	1272.22	24	0.02	1260.70
110(A″)	τCCCC (70)			18	0.40	558.10	16	0.24	1172.67
111(A″)	τCCCC (67)			6	0.04	41529.53	4	0.06	90554.10

ν, δ, γ and τ denote stretching, in plane bending, out of plane bending and torsion, respectively.
[a] PED data are taken from VEDA4.
[b] Scaled frequency.
[c] I_{IR} and I_{R}: Calculated infrared (km/mol) and Raman (Å/amu) intensities.

0.97764, 0.80° – 0.55° – 0.97711 and 5.57° – 3.26° – 0.99828 for BLYP/6-31G(d) and 0.10 Å – 0.07 Å – 0.97929, 0.80° – 0.55° – 0.97672 and 5.57° – 3.26° – 0.99828 for BP86/6-31G(d), respectively.

Vibrational studies

All the experimental and theoretical vibrational frequencies for the compound, along with corresponding vibrational assignments and intensities are given in Table 5. The experimental and simulated vibrational spectra are depicted in Figs. 4 and 5. All the computed frequency values presented in this paper were obtained within the harmonic approximation. This allows describing the vibrational motion in terms of independent vibrational modes, each of which is governed by a simple one-dimensional harmonic potential. The compound consists of 39 atoms, having 111 normal vibrational modes, and it belongs to the point group C_s. The 111 modes of vibrations account for the irreducible representations $\Gamma_v = 77A' + 34A''$ of the C_s point group. The assignments of vibrational modes for the investigated isomers have been provided by VEDA 4. The following are some of the important vibrational motions that were observed.

CH vibrations

In benzene related aromatic compounds, separate ring CH or CC fundamental modes of vibrations are possible. However, as with any complex molecules, vibrational interactions occur and these labels can only indicate the predominant vibrations. In the aromatic compounds, the CH stretchings normally occur in the region of 3100–3000 cm^{-1} [31]. CH stretching vibrations for 2-acetyl-5-chlorothiophene (ACT) group were observed at 3146 (IR) and 3103 (IR/R) cm^{-1} [23]. For the present compound, one CH stretching frequency of thiophene ring (ν_3) was observed at 3116 (R) cm^{-1}. This Raman value is consistent with our previously reported data [23]. But, the decrease in the band number and the data without IR are purely due to the impact of substitutions on the ring and change of the environment or state for the molecule. The CH stretchings belong to $\nu_{5,6,11}$, ν_{13} and ν_{14-15} modes were reported at 3096 (IR), 3095 (R) and 3076 (IR) for benzene rings, 3058 (R) for enone group and 3052 (IR), 3038 (R), 3025 (IR), 3008 (R) for double bond between benzene rings. This observation indicates that all the stretching vibrations are within the expected range. Also, these bands are consistent with previously reported data [32–38]. The corresponding computed theoretical values at 3108, 3100, 3098, 3076, 3065, 3059 and 3049 cm^{-1} show excellent agreement with the experimental data.

The CH in-plane bending vibrations usually occur in the region of 1300–1000 cm^{-1} while the CH out-of-plane bending modes generally occur in the region of 1000–710 cm^{-1} [36,37]. For ACT, the CH in-plane bending vibrations of thiophene were assigned in the region of 1275–1075 cm^{-1} while the CH out-of-plane bending modes were reported in the region of 900–800 cm^{-1} [23]. In the present work, the CH in-plane bands for pure benzene (ν_{26}, ν_{47}) and thiophene (ν_{34}, ν_{40}, ν_{53}) rings were reported at 1453 (R),

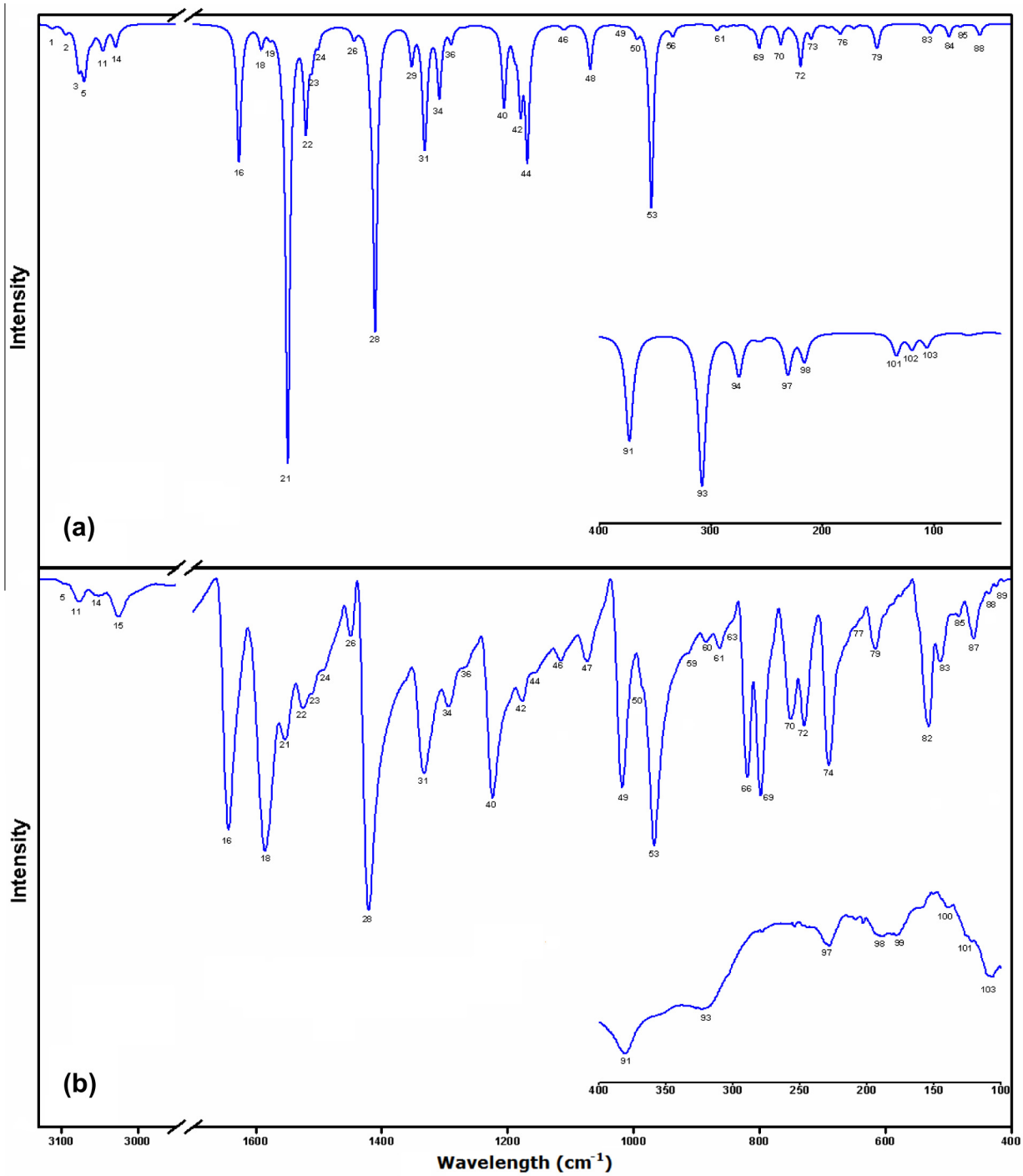

Fig. 4. (a) Theoretical and (b) experimental IR spectra for the compound.

1449 (IR), 1082 (R) cm^{-1} and 1294 (IR), 1224 (IR), 967 (IR/R) cm^{-1}, respectively. The mixed CH in-plane modes (ν_{31}, ν_{36}, ν_{46}) for benzene rings and enone group were recorded at 1333 (IR), 1327 (R), 1269 (IR) and 1116 (IR) cm^{-1}. In the IR spectrum, the mixed CH in-plane modes (ν_{42}) for benzene, thiophene and enone were assigned at 1176 cm^{-1} whereas some modes (ν_{39}, ν_{48}) were seen at 1228 (R), 1074 (IR) and 1060 (R) cm^{-1} for benzene and thiophene rings. Similar situations have been reported in the literature [32–38]. These modes were computed at 1444, 1332, 1308, 1289, 1210, 1205, 1179, 1110, 1076, 1068, 972 cm^{-1}.

The CH out-of-plane bands for pure enone (ν_{50}), benzene (ν_{57}, ν_{60}, ν_{66}) and thiophene (ν_{70}) groups were shown at 986 (IR) and, 919 (R), 886 (R), 885 (IR), 820 (IR) and 751 (IR) cm^{-1}, respectively. In the IR spectrum, the mixed CH out-of-plane bending vibrations for all groups except thiophene (ν_{69}, ν_{83}) was recorded at 798 and 531(IR) cm^{-1}. Similar situations have been reported in the literature [32–38]. The corresponding scaled values of these modes were predicted at 995, 924, 885, 813, 800, 766, 528 cm^{-1}.

Ring vibrations

In general, the ring CC stretching vibrations bands are of variable intensity. They are observed at 1625–1590, 1590–1575, 1540–1470, 1465–1430 and 1380–1280 cm^{-1} from the frequency ranges as the five bands [37]. In this compound, the C=C stretchings were assigned at 1585 (IR), 1526 (IR/R), 1494 (IR), 1493 (R) cm^{-1} for benzene rings (ν_{18}, ν_{22}, ν_{24}, ν_{25}), 1557 (R), 1554 (IR)

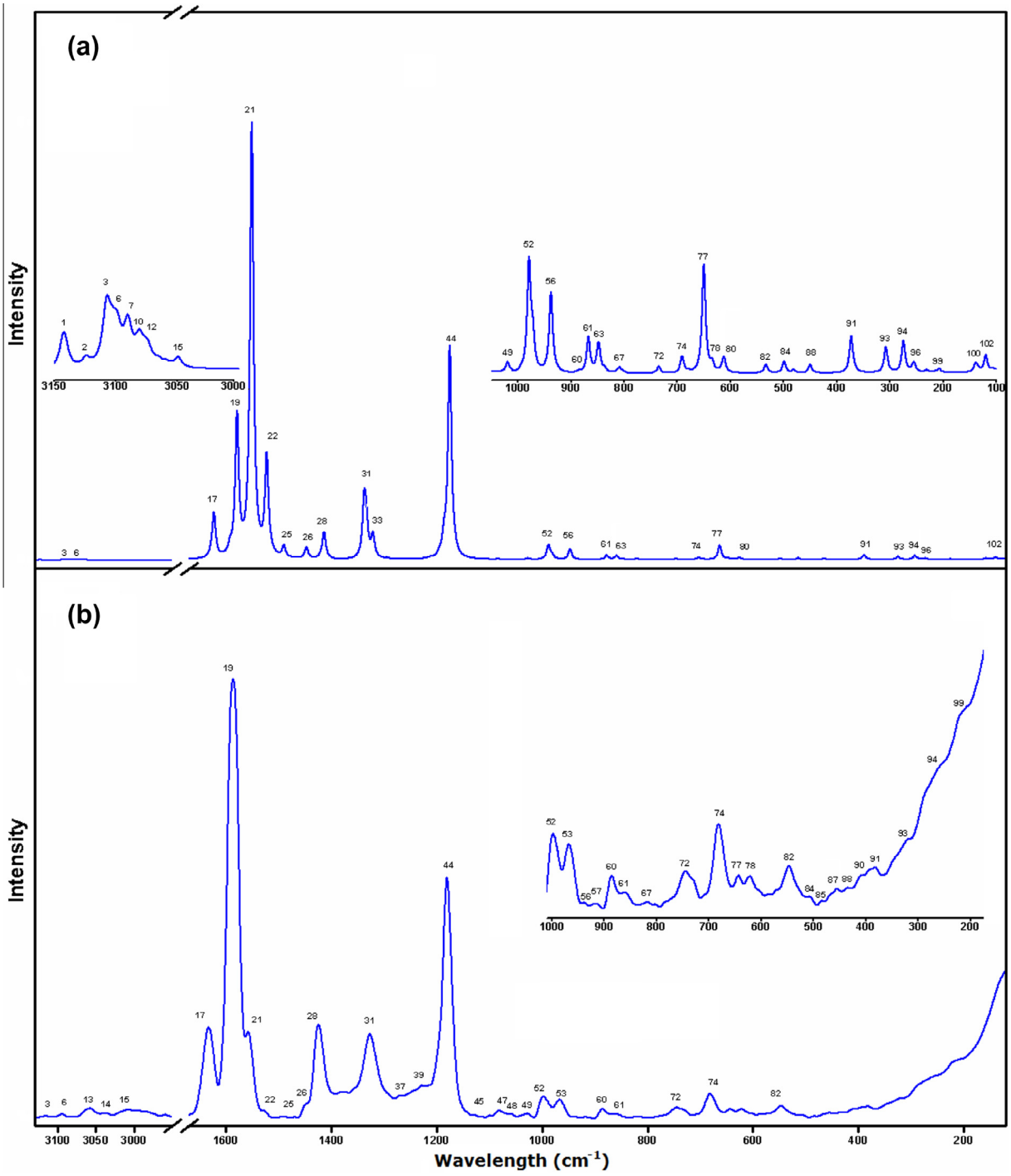

Fig. 5. (a) Theoretical and (b) experimental Raman spectra for the compound.

cm^{-1} for enone group (ν_{21}), 1511 (IR), 1424 (R), 1420 (IR) cm^{-1} for thiophene (ν_{23}, ν_{28}), 1633 (R), 1586 (R), 1269 (R) cm^{-1} for benzene rings/double bond groups ((ν_{17}, ν_{19}, ν_{37}). The predicted values at 1622, 1591, 1577, 1549, 1520, 1510, 1501, 1487, 1410, 1268 cm^{-1} are in excellent agreement with experimental data. All the stretching vibrations are found in the expected range and are in good agreement with the literature values [32–38].

The ring in-plane (ν_{52}, ν_{78}, ν_{90}) and out-of-plane bending (ν_{89}) vibrations were observed at 998 (R), 622 (R), 407 (R) cm^{-1} and 424 (IR) cm^{-1} for benzene rings, respectively. The ring out-of-plane bending band (ν_{87}) of thiophene was assigned at 460 (IR), 455 (R) cm^{-1}. The ring in-plane bending mode (ν_{56}) for thiophene/enone is shown at 936 (R) cm^{-1}. The ring in-plane and out-of-plane bending modes were assigned at 864 (IR), 861 (R), 818 (R), 318 (IR/R), 228 (IR) cm^{-1} and 221 (R), 176 (IR) cm^{-1} for all groups except thiophene (ν_{61}, ν_{67}, ν_{93}, ν_{97}, ν_{99}), respectively. The bands at 616 (IR), 547 (R), 485 (R), 484 (IR), 436 (IR), 433 (R), 125 (IR) cm^{-1} are reported as mixed ring in-plane (ν_{79}, ν_{82}, ν_{85}, ν_{88}, ν_{101}) modes for all groups, respectively. These modes were calculated at 979, 937, 867, 809, 634, 615, 533, 481, 452, 450, 397, 395, 307, 231, 207, 134 cm^{-1}.

Carbonyl vibrations

The carbonyl stretch of acetyl for ACT was reported at 1654/1651 cm^{-1} in IR/Raman spectra [23]. The CO stretch of the

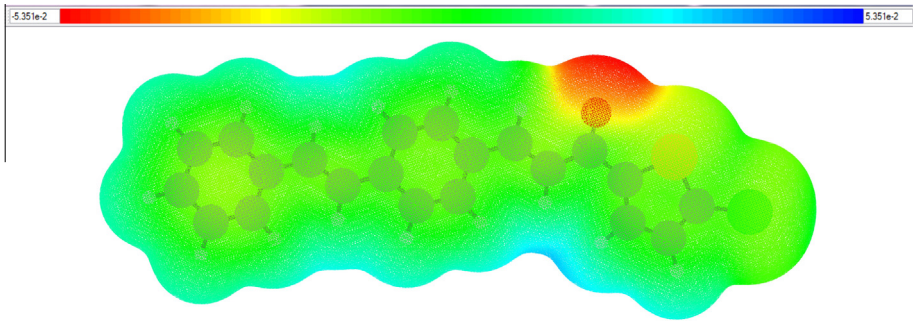

Fig. 6. Molecular electrostatic potential diagram of the *cis–trans–trans* isomer (isovalue = 0.0004) computed using the BLYP/6-31G(d) method in the gas phase.

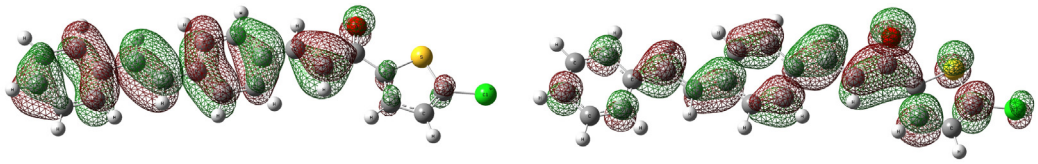

Fig. 7. Density plot of the HOMO and LUMO (contour value 0.02) of the *cis–trans–trans* isomer computed using the BLYP/6-31G(d) method in the gas phase.

compound (ν_{16}) was assigned to the observed very strong band at 1643 cm^{-1} in IR spectrum. The shift and disappear of Raman band are purely due to the effect of bonding 4-styryl-benzaldehyde molecule instead of a methyl group to CO group. The same vibration was calculated at 1626 cm^{-1}. The calculated value is in good agreement with the experimental data. These assignments are also in good agreement with the literature values [35,38–40]. The observed band 745/729 (R/IR) cm^{-1} can be assigned to the carbonyl group bending (ν_{72}). The predicted value at 735 cm^{-1} is in excellent agreement with experimental data.

Other vibrations

The CS stretch vibrations (ν_{74}/ν_{77}) were reported at 690 (IR), 681 (R) / 645 (IR), 644 (R) cm^{-1}. These modes were computed as 691/650 cm^{-1}. These vibrations are also reported in the literature [23,41]. The IR (Raman) bands at 513 (506) cm^{-1} were assigned to CCl stretching mode (ν_{84}) which correspond to the literature data [23,33,38,41]. The predicted value at 499 cm^{-1} is in excellent agreement with experimental data. The CCl in-plane mode vibration frequency appears at 274 cm^{-1} in the calculated value and experimental Raman band occurs at 260 cm^{-1}. The CCl out-of-plane mode vibration band appear at 138 cm^{-1} in the experimental IR and calculated frequency at 139 cm^{-1}. The torsion modes were in the low frequency region which corroborate with our theoretical findings. Vibrational modes in the low wavenumber region of the spectrum contain contributions of several internal coordinates and their assignment is a reduction approximation to one of two of the internal coordinates. All other vibrations are collected in Table 5.

NBO and molecular orbital analysis

We are interested in the nature of bonding of the atoms in the heteroatom ring and the C6B═C7B double bond in the *cis–trans–trans* form. The NBO data is collected in Table SI 1 (SI; Supplementary information). The double bond character of the C1B═C2B, C3B═C4B, C6B═C7B and C14B═C15B bonds are confirmed. The molecular electrostatic potential (MEP) of the same form is displayed in Fig. 6. The high electron density on oxygen of the carbonyl group is clearly observed.

Fig. 7 illustrates the density plot of the highest occupied molecular orbital (HOMO) and lowest unoccupied molecular orbital (LUMO) of the *cis–trans–trans* isomer plotted with a contour value of 0.02. These frontier orbitals determine the way the molecule interacts with other species. It can be observed from Fig. 7 that the HOMO is delocalized on all the atoms except for sulfur and mainly on the double bonds while the LUMO is delocalized over the entire compound, especially oxygen and sulfur atoms. The HOMO–LUMO gap is 1.98 eV. The laser used for Raman analysis in the present study is 2.33 eV and therefore, electronic excitement due to Raman laser may be possible.

Conclusions

The experimental, theoretical structural and vibrational investigations of (2*E*)-1-(5-chlorothiophen-2-yl)-3-{4-[(*E*)-2-phenylethenyl]phenyl}prop-2-en-1-one are successfully confirmed by FT-IR, Raman, single-crystal XRD and quantum chemical computations. Any differences observed between the experimental and computed values may be due to the fact that the computations were performed for a single molecule in the gas phase, whereas the experimental values in the solid phase were recorded in the presence of intermolecular interactions. To summarize, the following conclusions can be drawn:

(1) The compound crystallizes in the triclinic space group *P*-1 and the conformation about the O/S atoms and two C═C bonds of the structure are the *cis–trans–trans* form.
(2) It is worth to note that the compound has a large dipole moment (5.6 Debye) and this is an essential criterion for drug-receptor interaction [42].
(3) The following RMSD and MAD values (IR/R) are found for the experimental and theoretical vibrational wavenumbers of the *cis–trans–trans* form: 11/12 and 8/9 cm^{-1} for BLYP/6-31G(d) and 11/12 and 9/10 cm^{-1} for BP86/6-31G(d). Also, the R^2 values for IR/R are found to be 0.99978/0.99980 for BLYP/6-31G(d) and 0.99977/0.99979 for BP86/6-31G(d).
(4) The computations using the BLYP and BP86 functionals with the 6-31G(d) basis set are reliable and complement the understanding of vibrational spectra and structural parameters of the investigated compound as monomer. Also, BLYP is slightly better as a functional than BP86.

Acknowledgements

C.P. and M.T., L.R. and P.R. and M.B. acknowledge the facilities from Dumlupinar University, University of Mauritius and Ege University, respectively. C.S.C.K. thanks to Universiti Sains Malaysia (USM) for postdoctoral research fellowship (2013–2015). C.K.Q, C.S.C.K. and H.K.F. thank Malaysian Government and USM for Research University Individual Grant (1001/PFIZIK/811278) and Fundamental Research Grant Scheme (FRGS) (203/PFIZIK/6711411). The authors extend their appreciation to the Deanship of Scientific Research at King Saud University for the research group Project No. RGP VPP-207.

Appendix A. Supplementary data

Supplementary data associated with this article can be found, in the online version, at http://dx.doi.org/10.1016/j.saa.2015.04.022.

References

[1] K.J. Jarag, D.V. Pinjari, A.B. Pandit, G.S. Shankarling, Ultrason. Sonochem. 18 (2) (2011) 617.
[2] T. Vamakawa, H. Kagechika, E. Kawachi, Y. Hashimoto, K. Shudo, J. Med. Chem. 33 (1990) 1430.
[3] V.K. Ahluwalia, L. Nayal, N. Kaila, S. Bala, A. Tahim, Indian J. Chem. 26 (B) (1987) 384.
[4] A.K. Bhatt, R.P. Bhamaria, M.R. Patel, R.A. Bellare, C.V. Deliwala, Indian J. Chem. 10 (1972) 694.
[5] S. Mucherjee, V. Kumar, A.K. Prasad, H.G. Raj, M.E. Brakhe, C.E. Olsen, S.C. Jain, V.P. Parmar, Bio-org Med. Chem. 9 (2001) 337.
[6] S.A. Indyah, H. Timmerman, M. Samhoedi, D. Sastronami, H. Sugiyanto, V.D. Goot, Eur. J. Med. Chem. 35 (2000) 449.
[7] M. Chen, S.B. Christensen, L. Zhai, M.H. Rasmussen, T.G. Theander, S. Frokjaer, B. Steffensen, J. Davidson, A. Kharazmi, J. Infect. Dis. 176 (1997) 1327.
[8] V. Tomar, G. Bhattacharjee, K. Kamaluddina, Bioorg. Med. Chem. Lett. 17 (2007) 5321–5324.
[9] D. Bag, S. Ramar, M.S. Degani, Med. Chem. Res. 18 (2009) 309–316.
[10] T.D. Tran, T.T. Nguyen, T.H. Do, T.N. Huynh, C.D. Tran, K.M. Thai, Molecules 17 (2012) 6684–6696.
[11] A.M. Asiri, H.M. Marwani, K.A. Alamry, M.S. Al-Amoudi, S.A. Khan, S.A. El-Daly, Int. J. Electrochem. Sci. 9 (2014) 799–809.
[12] J.P. Jasinski, A.E. Pek, C.S. Chidan Kumar, H.S. Yathirajan, A.N. Mayekar, Acta Cryst. E 66 (2010) o1717.
[13] G. Dutkiewicz, C.S. Chidan Kumar, H.S. Yathirajan, B. Narayana, M. Kubicki, Acta Cryst. E 66 (2010) o1139.
[14] W.T.A. Harrison, C.S. Chidan Kumar, H.S. Yathirajan, A.N. Mayekar, B. Narayana, Acta Cryst. E 66 (2010) o2479.
[15] C. Nithya, N. Santhanamoorthi, P. Kolandaivel, K. Senthilkumar, J. Phys. Chem. 115 (2011) 6594–6602.
[16] C.S.C. Kumar, W.S. Loh, C.W. Ooi, C.K. Quah, H.K. Fun, Molecules 18 (2013) (2011) 11996–12011.
[17] C.S.C. Kumar, W.S. Loh, C.W. Ooi, C.K. Quah, H.K. Fun, Molecules 18 (2013) 12707–12724.
[18] C.S.C. Kumar, H.K. Fun, C. Parlak, L. Rhyman, P. Ramasami, M. Tursun, S. Chandraju, C.K. Quah, Spectrochim. Acta A 132 (2014) 174–182.
[19] M.J. Frisch, G.W. Trucks, H.B. Schlegel, G.E. Scuseria, M.A. Robb, J.R. Cheeseman, G. Scalmani, V. Barone, B. Mennucci, G.A. Petersson, H. Nakatsuji, M. Caricato, X. Li, H.P. Hratchian, A.F. Izmaylov, J. Bloino, G. Zheng, J.L. Sonnenberg, M. Hada, M. Ehara, K. Toyota, R. Fukuda, J. Hasegawa, M. Ishida, T. Nakajima, Y. Honda, O. Kitao, H. Nakai, T. Vreven, J.A. Montgomery, Jr., J.E. Peralta, F. Ogliaro, M. Bearpark, J.J. Heyd, E. Brothers, K.N. Kudin, V.N. Staroverov, R. Kobayashi, J. Normand, K. Raghavachari, A. Rendell, J.C. Burant, S.S. Iyengar, J. Tomasi, M. Cossi, N. Rega, J.M. Millam, M. Klene, J.E. Knox, J.B. Cross, V. Bakken, C. Adamo, J. Jaramillo, R. Gomperts, R.E. Stratmann, O. Yazyev, A.J. Austin, R. Cammi, C. Pomelli, J.W. Ochterski, R.L. Martin, K. Morokuma, V.G. Zakrzewski, G.A. Voth, P. Salvador, J.J. Dannenberg, S. Dapprich, A.D. Daniels, Ö. Farkas, J.B. Foresman, J.V. Ortiz, J. Cioslowski, D.J. Fox, Gaussian 09, Revision A.1, Gaussian Inc., Wallingford CT, (2009).
[20] R.D. Dennington, T.A. Keith, J.M. Millam, GaussView 5.0.8, Gaussian Inc., (2008).
[21] H.K. Fun, S. Chantrapromma, P.S. Patil, S.M. Dharmaprakash, Acta Cryst. E 64 (2010) o1720–1721.
[22] Z. Ngaini, S.M.H. Fadzillah, H. Hussain, I.A. Razak, H.K. Fun, Acta Cryst. E 65 (2010) o1301–1302.
[23] C.S.C. Kumar, C. Parlak, H.K. Fun, M. Tursun, G. Keşan, S. Chandraju, C.K. Quah, Spectrochim. Acta A 127 (2014) 67–73.
[24] A.P. Scott, L. Radom, J. Phys. Chem. 100 (1996) 16502–16513.
[25] M.H. Jamróz, Spectrochim. Acta A 114 (2013) 220–230.
[26] Ö. Alver, C. Parlak, Vib. Spectrosc. 54 (2010) 1–9.
[27] M. Tursun, G. Keşan, C. Parlak, M. Şenyel, Spectrochim. Acta A 114 (2013) 668–680.
[28] A.E. Reed, R.B. Weinstock, F. Weinhold, J. Chem. Phys. 83 (1985) 735–746.
[29] A.E. Reed, L.A. Curtiss, F. Weinhold, Chem. Rev. 88 (1988) 899–926.
[30] C. Parlak, J. Mol. Struct. 966 (2010) 1–7.
[31] Y.R. Sharma, Elementary Organic Spectrocopy – Principles and Chemical Applications, S. Chand & Company Ltd., New Delhi, 1994.
[32] W. Huang, X.H. Zhang, L.Y. Wang, G.H. Zhai, Z.Y. Wen, Z.X. Zhang, J. Mol. Struct. 977 (2010) 39–44.
[33] C.S.C. Kumar, H.K. Fun, M. Tursun, C.W. Ooi, S. Chandraju, C.K. Quah, C. Parlak, Spectrochim. Acta A 124 (2014) 595–602.
[34] H. Takashima, K. Endo, M. Ito, H. Takeuchi, T. Egawa, S. Konaka, J. Mol. Struct. 478 (1999) 13–22.
[35] R. Nithya, N. Santhanamoorthi, P. Kolandaivel, K. Senthilkumar, J. Phys. Chem. A 115 (2011) 6594–6602.
[36] J. Mohan, Organic Spectroscopy – Principle and Applications, second ed., Narosa Publishing House, New Delhi, 2001.
[37] G. Varsanyi, Vibrational Spectra of Benzene Derivatives, Academic Press, New York, 1969.
[38] S. Prabu, R. Nagalakshmi, J. Balaji, P. Srinivasan, Mater. Res. Bull. 50 (2014) 446–453.
[39] H.L. Hegert, E.F. Kurth, J. Am. Chem. Soc. 75 (1953) 1622.
[40] A. Perjéssy, Chem. Zvesti 23 (1969) 905–915.
[41] G. Socrates, Infrared and Raman Characteristic Group Frequencies Tables and Charts, third ed., Wiley, Chichester, 2001.
[42] E.J. Lien, Z.-R. Guo, R.-L. Li, C.-T. Su, J. Pharm. Sci. 71 (1982) 641–655.